IOP Conf. Series: Materials Science and Engineering **1345** (2026) 012030 doi:10.1088/1757-899X/1345/1/012030

Characterization of 850 nm Power Over Fiber Converter at Cryogenic Temperatures

Cody Kaminsky[1], **Ethan Huang**[1], **Lukas Graber**[1]

[1]Electrical and Computer Engineering, Georgia Institute of Technology, Atlanta, USA

E-mail: ethanhuang@gatech.edu

Abstract. Power over Fiber (PoF) technology, which enables the transmission of electrical power via optical fibers, has gained significant traction across diverse applications, including telecommunications, aerospace, and high-voltage power distribution. Its unique advantages—such as intrinsic electrical isolation, immunity to electromagnetic interference, and excellent thermal insulation—make it particularly valuable in environments where conventional power delivery poses risks or limitations. A new application for PoF is its use in cryogenic environments, where the low thermal conductivity of optical fibers allows them to bridge extreme temperature gradients without significant heat transfer. This paper builds upon prior research exploring PoF systems operating under cryogenic conditions. This paper will present a study of system performance across a range of temperatures, capturing key operational trends and performance metrics as a function of temperature. Our results highlight critical insights into power conversion efficiency, thermal stability, and optical-to-electrical energy transfer characteristics at low temperatures. The findings are instrumental in guiding the future design and optimization of PoF systems for cryogenic and extreme environments, paving the way for more efficient, reliable, and high-power solutions in next-generation scientific and industrial applications.

1 Introduction

Power over fiber (PoF) was first proposed as a means of powering a telephone line [1]. It operated at 2 mW with an efficiency of 35 percent. Since then, many new applications for PoF have emerged and reached widespread adoption in many disciplines. In 2023, Wada et al demonstrated a system that transmitted 1 W of power over 10 km while simultaneously providing communication [2]. PoF has several benefits, including thermal isolation, electrical isolation, and immunity against electromagnetic interference (EMI). These properties make it ideal for telecommunications, high-noise, and high-voltage systems [3–6].

The electrical isolation property makes PoF perform well when interacting with a high-voltage system that requires isolation between the sensor and the system it measures. This is also the case for gate drivers and other electronics that aid in controlling the high-voltage system. Since telecommunication systems are widespread and often operate in noisy environments, PoF can be of great value. The electrical isolation it provides isolates any surges or lightning strikes [7] while also eliminating the need for a local power supply in certain telecommunication devices [8]. In addition, the low thermal conductivity of glass fibers allows them to span large temperature gradients without acting as a heat leak into a temperature-controlled area. Thermal isolation will enable PoF devices to be used in harsh environments while maintaining temperature regulation.

Recent work from M. Torti et al. investigated the performance of a similar PoF system at three temperatures: 300 K, 87 K, and 77 K. The study noted a decline in performance when the temperature lowers [9]. Building on this foundation, this paper offers a more granular analysis by characterizing the PoF system across higher resolution measurements, from 300 K to 100 K in 25 K increments. The intention of which is to find trends of the characteristics of the device as a function of temperature to better understand how to improve them in the future.

2 Methodology

The Broadcom AFBR-POC406L Optical Power Converter (OPC) was selected for characterization across a temperature range of −175 °C to 25 °C. This temperature range was selected because it reflects the conditions most relevant to cryogenic power electronics, with future work aimed at extending the characterization to even lower temperatures.

The device operates within the optical wavelength range of 800 nm to 850 nm. It is specified to deliver a peak power of 0.6 W (93 mA at 6.5 V) under an optical input power of 1.0 W. To ensure compatibility, a Broadcom AFBR-POL2120 laser source with a nominal emission wavelength of 809 nm and a rated output of 2 W was chosen. However, for this paper, the optical output power was regulated at 1 W.

The OPC was placed inside an EC13 environmental chamber (see Figures 1,2), which regulated the temperature using liquid nitrogen (LN2). This means the lowest temperature that the chamber can achieve will be slightly above the boiling point of LN2 of 77 K at sea level.

For our characterizations, the chamber was programmed to regulate the temperature at the following setpoints: 25 °C, 0 °C, −25 °C, −50 °C, −75 °C, −100 °C, −125 °C, −150 °C, −175 °C. At each temperature, the system was allowed to stabilize within ±5 °C of the target, followed by a five-minute soaking period. These parameters were chosen based on the expected accuracy of the chamber's control system. During this time, the optical laser and OPC were kept off to prevent the device from increasing the temperature in the chamber.

Figure 1: Experimental setup internal to the EC13 environmental chamber

Figure 2: EC13 environmental chamber with front experimental setup enclosed

The device's I-V curve was measured at each temperature set point to characterize the OPC's performance. This was achieved using a constant current driver acting as a variable resistive load. A Python routine, interfaced with a National Instruments NI-DAQ system, incrementally swept the driver's reference voltage from 0 V until the short-circuit current of the Broadcom OPC was found. From the resulting I-V curves, the peak power, open-circuit voltage, short-circuit current, and fill factor were extracted to characterize the device's behavior across the thermal range. As illustrated in the system diagram (Figure 3), the constant current driver and laser source were located outside the environmental chamber, ensuring that only the OPC was exposed to thermal variation. The I-V curve was measured six times at each temperature set-point: three while decreasing and three while increasing. This approach accounted for both measurement variability and potential thermal hysteresis effects.

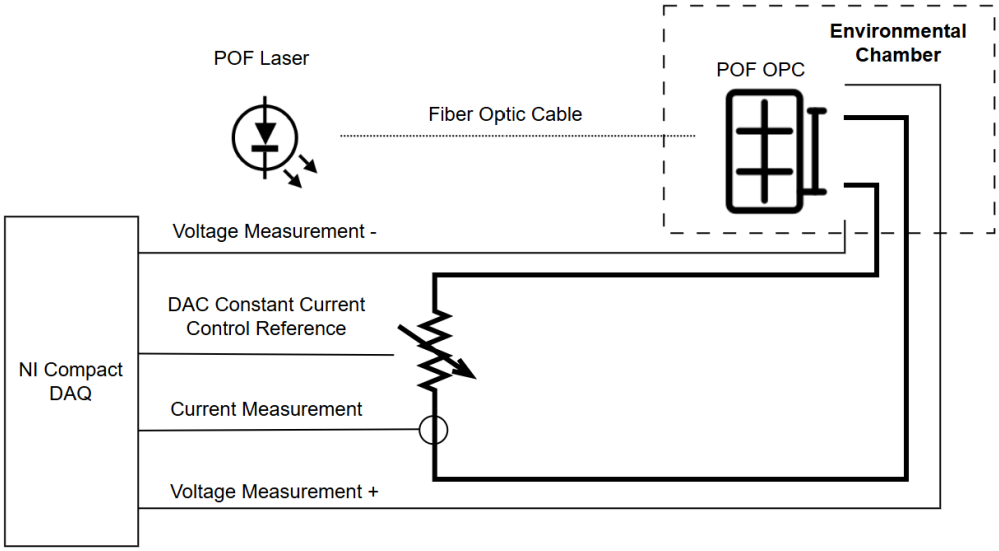

Figure 3: System diagram of the test setup used to characterize the optical power converter

3 Results

To validate the experimental setup, an initial I-V curve was measured at 25 °C and compared against the datasheet for the Broadcom OPC. The general shape, open circuit, and short circuit currents closely align with the datasheet. Figure 4 shows that the peak power is 0.602 W, occurring at 6.488 V and 92.8 mA. This is well within the 3 percent of the datasheet's nominal values (0.6 W, 93 mA at 6.5 V). The measured characteristic error is negligible, confirming the experimental setup's reliability.

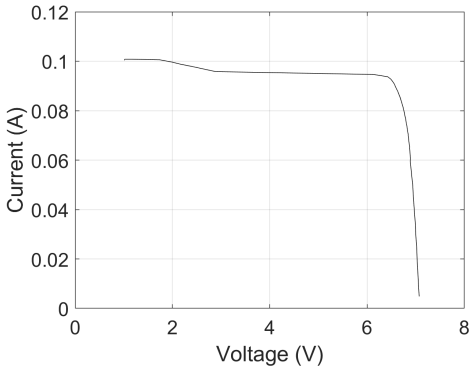

Figure 4: I-V curve of the power converter at 25C

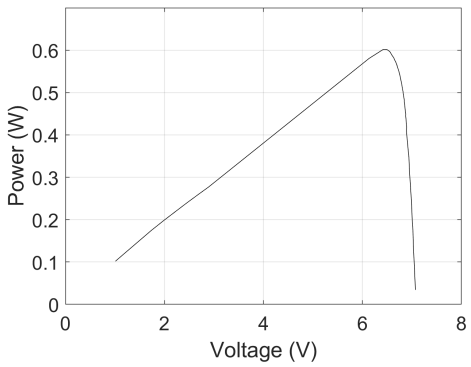

Figure 5: P-V curve of the power converter at 25C

Figures 6 and 7 show the open-circuit voltage and short-circuit currents from the measured I-V curves. The open-circuit voltage exhibits a monotonic increase as temperature decreases, reaching a maximum of 8.1 V at approximately −150 °C. Below this temperature, the voltage trend decreases. In contrast, the short-circuit current remains stable across the temperature range, varying between 100 mA and 110 mA from −175 °C to 25 °C.

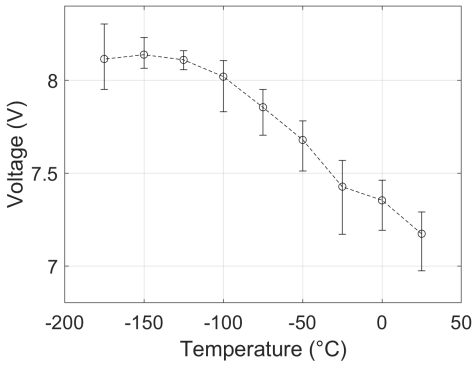

Figure 6: Open-circuit voltage as a function of temperature

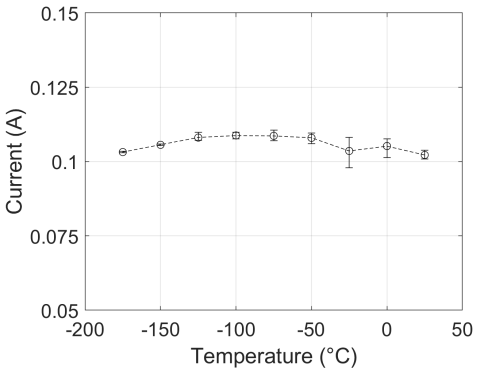

Figure 7: Short-circuit current as a function of temperature

The OPC peak power output was calculated by identifying the maximum product of the measured current and voltage values from the I-V curves. Intuitively, one might expect the peak power to occur at the temperature corresponding to the highest open-circuit voltage and short-circuit current (−150 °C). Yet, the measured maximum peak power output was at −50 °C. This suggests that the open-circuit voltage and short-circuit current did not significantly impact the peak power. Instead, the fill factor seemed to be a more accurate indicator. The fill factor was found by the ratio of the area under the I-V curve to the product of the open-circuit voltage and short-circuit current. Figure 9 shows that the fill factor follows a similar trend to peak power (Figure 8). As the temperature decreases, the fill factor increases monotonically until −50 °C, then decreases rapidly, just as peak power does. The underlying mechanism is beyond the scope of this study and will be addressed in future work.

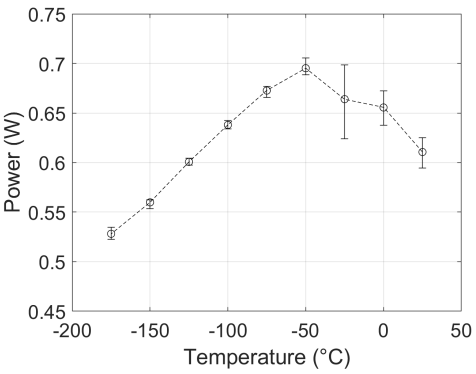

Figure 8: Peak power as a function of temperature

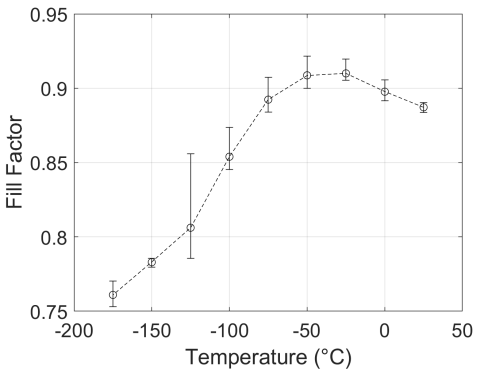

Figure 9: Fill factor as a function of temperature

Extrapolating the trends of the open-circuit voltage and fill factor, the peak power of the OPC will decline below −175 °C. Although the open-circuit voltage increases to approximately −150 °C, partially compensating for the declining fill factor beyond −50 °C, both metrics decline beyond this point. At the same time, the short-circuit current remains relatively stable. This suggests that the peak power will likely continue to decrease past −175 °C. While this does not mean the OPC can not be used at temperatures lower than −175 °C, it provides insight into the optimal temperature range for the device. Furthermore, M. Torti et al. support this notion with numerical data. In their testing, the system worked until 7 K at a low efficiency of 15 percent [9]. Comparatively, the efficiency of the PoF OPC at −175 °C in this paper's results is at a peak efficiency of 53 percent.

To better understand the observed reduction in fill factor—and, by extension, peak power—the voltage and current at the maximum power point were further examined. Figures 10 and 11 compare the voltage at peak power to open-circuit voltage and the current at peak power to short-circuit current. Figure 11 shows that the offset from short-circuit current to the current at peak power does not vary much

across the thermal range, which indicates that the device's current over temperature is not a significant determining factor of the fill factor. In contrast, the voltage at peak power vastly diverges from the open-circuit voltage across the temperature range. The OPC's voltage cannot be sustained for a given current.

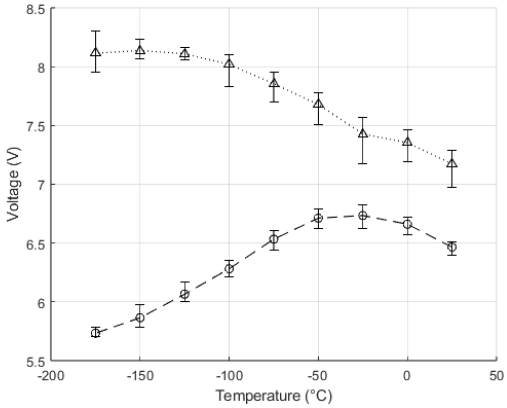

Figure 10: Open-circuit voltage and voltage at peak power as a function of temperature

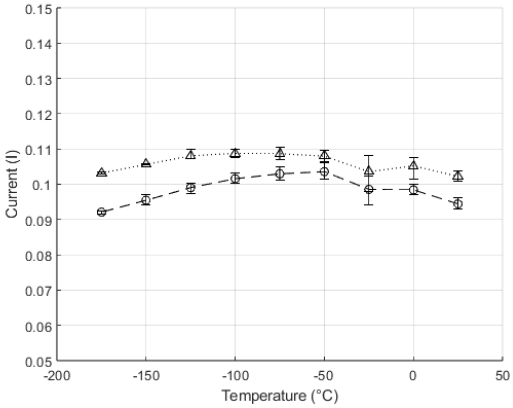

Figure 11: Short-circuit current and current at peak power as a function of temperature

As indicated by the error bars, the small differences between increasing and decreasing sweeps were consistent with measurement error and did not suggest a systematic hysteresis effect.

4 Applications in Cryogenic Power Electronics

The research area of cryogenic power electronics is a rapidly evolving and relatively new field that can lead to higher power density and greater efficiency. An interesting application of cryogenic power electronics is in electric transportation, specifically in aircraft. In this application, minimizing the size and weight of the electrical system is of utmost importance. Electric motors, generators, wiring harnesses, semiconductors, and passive electronic components can significantly improve power density and efficiency.

Specifically, the efficiency of a motor increases from 37.6 % at 300 K to 63.2 % at 77 K [10], demonstrating the potential for substantial performance gains in low-temperature environments. For silicon devices, electron mobility increases from $650\,\mathrm{cm^2\,V^{-1}\,s^{-1}}$ at 300 K to approximately $1000\,\mathrm{cm^2\,V^{-1}\,s^{-1}}$ at 77 K, for a doping concentration of $N_\mathrm{d} = 2 \times 10^{17}\,\mathrm{cm^{-3}}$ [11]. Similarly, GaN devices show an increase in electron mobility from $1067\,\mathrm{cm^2\,V^{-1}\,s^{-1}}$ at 300 K to $2885\,\mathrm{cm^2\,V^{-1}\,s^{-1}}$ at 77 K [11]. To operate these devices and systems at cryogenic temperatures, they must be supported by devices at ambient temperatures. This opens up the possibility for using PoF as a means to power sensors or gate-drivers for semiconductors or motors.

5 Conclusion and Future Work

The Broadcom OPC was determined to work sufficiently well down to −175 °C with a minimum peak power of 0.53 W, a 12 percent reduction from its rated value at room temperature. This amount of power is acceptable enough to power sensors, gate-drivers, or other cryogenic electronics applications. From the I-V curve and subsequent analysis, the fill-factor was the most significant influence for the device's peak power at a given temperature, despite the open-circuit voltage changing by up to 14 percent across the temperature range. Further investigation showed that the voltage at peak power affected the fill factor most significantly, as it diverged from the open-circuit by 2.4 V at −175 °C compared to 0.7 V at −25 °C.

The methodology could be improved to measure the I-V curve more precisely, and a cryocooler can be used to decrease temperatures past the boiling point of LN2. Future work should be done to understand the temperature-dependent behavior of the fill factor, which remains the key determinant of peak power, but whose underlying mechanism is not yet investigated. In parallel, work should be done to determine how to increase the fill factor to maximise OPC performance in cryogenic environments. Since the OPC performed well in the cryogenic conditions, applications of this device should continue to be investigated to make use of POF technologies.

References

[1] R. C. Miller and R. B. Lawry, "Optically powered speech communication over a fiber lightguide," Bell System Technical Journal, vol. 58, no. 7, pp. 1735–1741, Sep. 1979, doi: 10.1002/j.1538-7305.1979.tb02280.x.

[2] M. Wada, K. Kurokawa, T. Matsui, H. Iida, and K. Nakajima, "High-efficiency and long-distance power-over-fibre transmission using a 125-μm cladding diameter 4-core fibre," IET Conference Proceedings., vol. 2023, no. 34, pp. 84–87, Nov. 2023, doi: 10.1049/icp.2023.1855.

[3] X. Zhang et al., "A gate drive with power over Fiber-Based isolated power supply and comprehensive protection functions for 15-KV SIC MOSFET," IEEE Journal of Emerging and Selected Topics in Power Electronics, vol. 4, no. 3, pp. 946–955, Jun. 2016, doi: 10.1109/jestpe.2016.2586107.

[4] N. J. Yan, N. J. Wang, N. Y. Lu, N. J. Jiang, and N. H. Wan, "Novel wireless sensor system based on power-over-fiber technique," 2022 20th International Conference on Optical Communications and Networks (ICOCN), vol. 3, pp. 1–3, Jul. 2015, doi: 10.1109/icocn.2015.7203710.

[5] F. V. B. De Nazare and M. M. Werneck, "Temperature and current monitoring system for transmission lines using power-over-fiber technology," May 01, 2010, pp. 779–784. doi: 10.1109/imtc.2010.5488198.

[6] F. B. F. Pinto et al., "Power-over-fiber-based optical wireless communication systems towards 6G," Journal of Optical Communications and Networking, vol. 16, no. 8, p. D86, Jun. 2024, doi: 10.1364/jocn.522583.

[7] F. R. Bassan et al., "Power-over-Fiber LPIT for voltage and current measurements in the medium voltage distribution networks," Sensors, vol. 21, no. 2, p. 547, Jan. 2021, doi: 10.3390/s21020547.

[8] J. D. Lopez-Cardona, C. Vazquez, D. S. Montero, and P. C. Lallana, "Remote optical powering using fiber optics in hazardous environments," Journal of Lightwave Technology, vol. 36, no. 3, pp. 748–754, Nov. 2017, doi: 10.1109/jlt.2017.2776399.

[9] M. Torti et al., "Results from Cryo-PoF: Power over fiber for fundamental and applied physics at cryogenic temperature," Nuclear Instruments and Methods in Physics Research Section a Accelerators Spectrometers Detectors and Associated Equipment, vol. 1068, p. 169753, Aug. 2024, doi: 10.1016/j.nima.2024.169753.

[10] F. J. M. Dias, G. G. Sotelo, and R. De Andrade Júnior, "Improving the induction motor power density by its operation at liquid nitrogen bath," Cryogenics, vol. 127, p. 103551, Sep. 2022, doi: 10.1016/j.cryogenics.2022.103551.

[11] Y. Liao et al., "Review of semiconductor devices and other power electronics components at cryogenic temperature," iEnergy, vol. 3, no. 2, pp. 95–107, Jun. 2024, doi: 10.23919/ien.2024.0014.